Ice-Tethered Profiler Measurements of Dissolved Oxygen under Permanent Ice Cover in the Arctic Ocean

M.-L. TIMMERMANS

Department of Geology and Geophysics, Yale University, New Haven, Connecticut

R. KRISHFIELD

Department of Physical Oceanography, Woods Hole Oceanographic Institution, Woods Hole, Massachusetts

S. LANEY

Biology Department, Woods Hole Oceanographic Institution, Woods Hole, Massachusetts

J. TOOLE

Department of Physical Oceanography, Woods Hole Oceanographic Institution, Woods Hole, Massachusetts

(Manuscript received 26 January 2010, in final form 11 June 2010)

ABSTRACT

Four ice-tethered profilers (ITPs), deployed between 2006 and 2009, have provided year-round dissolved oxygen (DO) measurements from the surface mixed layer to 760-m depth under the permanent sea ice cover in the Arctic Ocean. These ITPs drifted with the permanent ice pack and returned 2 one-way profiles per day of temperature, salinity, and DO. Long-term calibration drift of the oxygen sensor can be characterized and removed by referencing to recently calibrated ship DO observations on deep isotherms. Observed changes in the water column time series are due to both drift of the ITP into different water masses and seasonal variability, driven by both physical and biological processes within the water column. Several scientific examples are highlighted that demonstrate the considerable potential for sustained ITP-based DO measurements to better understand the Arctic Ocean circulation patterns and biogeochemical processes beneath the sea ice.

1. Introduction

Dissolved oxygen (DO) has been used to examine marine primary production and respiration in the Arctic Ocean, where water column DO patterns are consistent with those expected from light-driven seasonal trends in primary production by phytoplankton and ice algae (Codispoti and Richards 1971; Cota et al. 1996; Pomeroy 1997; Sherr and Sherr 2003; Codispoti et al. 2005). Cota et al. (1996) found significant rates of photosynthetic production, evidenced by high-DO concentrations, well into the perennial ice-covered region of the Arctic Ocean's Canada Basin. The 1997–98 Surface Heat Budget of the Arctic Ocean (SHEBA)/Joint Ocean Ice Study (JOIS) project included upper-ocean measurements of DO under permanent ice cover in the Canada Basin over one annual period that indicated a level of primary productivity one order of magnitude higher in summer than that in winter, with large interannual variability likely resulting from biological activity (Sherr and Sherr 2003).

In addition to its biological importance, DO has been used extensively in the Arctic Ocean as a valuable tracer for examining water mass origins and dynamics (e.g., Kinney et al. 1970; McLaughlin et al. 2004; Falkner et al. 2005; Shimada et al. 2005; Woodgate et al. 2005; Itoh et al. 2007). Nutrient-rich Pacific-origin waters, for example, are characterized by low-DO values; Falkner et al. (2005) traced DO signatures in the vicinity of the North Pole and the shelf regions off Ellesmere Island to infer the basin-scale circulation of Pacific waters. Itoh et al. (2007) used DO measurements to determine sources and pathways of water marked by anomalously high DO, deducing that it originates at the surface in the Eurasian

Corresponding author address: Mary-Louise Timmermans, Department of Geology and Geophysics, Yale University, New Haven, CT 06515.
E-mail: mary-louise.timmermans@yale.edu

DOI: 10.1175/2010JTECHO772.1

Basin and spreads into the Canadian Basin halocline (between the base of the surface mixed layer and about 200-m depth).

Recent Arctic sea ice and climate variability (e.g., Richter-Menge and Overland 2009; Nihoul and Kostianoy 2009) underscores the essential need for sustained, uninterrupted measurements of the Arctic Ocean's physical and biogeochemical environment. Loss of sea ice area and a longer growing season in the Arctic is accompanied by increased phytoplankton production (Arrigo et al. 2008). Arrigo et al. (2008) found that annual primary production in the Arctic increased by more than 15% between 2006 and 2007, the year of minimum summer sea ice extent. Sea ice loss is accompanied by sea ice thinning, which will likely also affect photosynthetic organisms living at and below the ice–ocean interface by providing them with more light, impacting both photosynthesis and subice biogeochemical cycles.

Over decadal time scales, global climate change may be contributing to the observed reduction in DO in lower-latitude oceans (e.g., Johnson and Gruber 2007; Mecking et al. 2008; Stramma et al. 2008). Observations and climate model predictions indicate that these declining DO levels can be attributed to ocean warming and subsequent changes in surface water solubility, changes in biological production, and dynamical ocean changes (Bopp et al. 2002; Stramma et al. 2008). In a warming and freshening Arctic Ocean (Proshutinsky et al. 2009), similar factors are likely also to be of relevance.

Considerable changes in ocean physical properties, photosynthesis, primary production, food webs, and biogeochemical cycles may take place unobserved in the hard-to-sample, ice-covered ocean environment. Consequently, innovative sampling approaches are needed. Ice-tethered profilers (ITPs) have proven to be an innovative way to return stable, high-quality measurements of ocean physical properties in permanently ice-covered regions (Krishfield et al. 2008a). Here, we show how ITPs are also an effective platform to obtain long-term measurements of DO over a large portion of the Arctic Ocean. These systems provide the high-latitude complement to the recent international joint Argo–Oxygen program documenting variations in DO concentrations in the upper ocean at lower latitudes (e.g., Gruber et al. 2009).

Here, we present continuous autonomous measurements of DO, temperature, and salinity under permanent sea ice from four ITPs drifting in the permanent sea ice pack in the Canada and Makarov Basins, between 2006 and 2009, over several seasonal cycles. In the next section, the instrumentation and data processing are described. In section 3, the scientific opportunities made possible by these systems are illustrated through an overview of the spatial and temporal distribution of dissolved oxygen and distinctive features. The results are summarized in section 4.

2. Methods

a. Ice-tethered profiler

The ITP is an automated profiling CTD instrument that returns frequent high vertical resolution measurements of upper-ocean temperature, salinity, and optionally DO beneath sea ice during all seasons for up to a 3-yr lifetime. The system includes a profiling vehicle that is deployed through a 25-cm-diameter hole drilled in perennial ice that is typically between 1.5 and 3 m thick. The profiler cycles vertically between around 7- and 760-m depth along a weighted tether below a surface buoy in the supporting ice floe. The standard profiler is equipped with the Sea-Bird Electronics (SBE) 41CP CTD sensor sampling at 1 Hz (systems with DO sensors sample at 0.8 Hz). The vehicle profiles at a speed of about 25 cm s^{-1}, so that the raw data have a vertical resolution of around 25 cm. ITP sensor data are transmitted from the profiler to the surface buoy via modem and are relayed to the shore via the Iridium satellite system. The ITP data are processed immediately upon receipt and preliminary products are made directly available online (http://www.whoi.edu/itp). Complete technical details of the ITP system are given in Krishfield et al. (2008a). Johnson et al. (2007) established appropriate sensor response correction methods to raw data from SBE 41CP CTDs mounted on ITPs.

b. Oxygen sensor

Four ITP systems (serial numbers 6, 13, 23, and 29) were additionally equipped with Sea-Bird Electronics DO sensors (SBE 43). This type of DO sensor is also currently being deployed on autonomous profiling floats in the lower latitudes as part of the Argo program (e.g., Riser and Johnson 2008). The SBE 43s are Clark-type electrochemical cells that measure the diffusion of oxygen molecules through a membrane (details are given in Sea-Bird Electronics, Inc. 2010a). The temperature-compensated signal of the SBE 43F DO sensor is a frequency output (F), and it is used in a continuously pumped mode [ITPs incorporate a continuously pumped CTD (SBE 41CP)]. In this case, the equilibration time of the sensor with the in situ oxygen concentration is a few seconds, depending on sensor characteristics.

c. Data processing

The first step in data processing is to apply a correction to sensor output F to account for mismatches between up and down profile data that have been observed

in SBE 43 sensor output, particularly for deep-ocean profiles ≳1000 m (Edwards et al. 2009). This hysteresis has been attributed to changes of the sensor's membrane permeability at high pressures, and it is corrected with a function of the time–pressure history of the sensor using the following algorithm (see Sea-Bird Electronics, Inc. 2010c):

$$F_1(i) = F(i) + F_{\text{offset}}, \tag{1}$$

$$F_2(i) = \{[F_1(i) + F_2(i-1)\mathcal{CD}] - F_1(i-1)\mathcal{C}\}/\mathcal{D}, \tag{2}$$

$$F_c(i) = F_2(i) - F_{\text{offset}}, \tag{3}$$

for $\mathcal{D} = 1 + H_1\{\exp[P(i)/H_2] - 1\}$, and $\mathcal{C} = \exp\{-[t(i) - t(i-1)]/H_3\}$. Here $P(i)$ is pressure at index i, t is time, and F_1 is the sensor frequency with the F_{offset} correction applied. Additionally, H_1 is the sensor-dependent amplitude of the hysteresis correction, H_2 is a curvature constant for hysteresis, and H_3 is a sensor-dependent time constant for hysteresis, all of which are provided by SBE. Last, F_2 is the hysteresis-corrected oxygen value and F_c is the hysteresis-corrected oxygen value with F_{offset} removed—a necessary step prior to computing oxygen concentration from frequency. The hysteresis correction is minor for the ITP profiles to about 760 m, and adjusts values by no more that about 0.3% higher at 760 m, with no discernable difference shallower than about 300 m.

The concentration of DO (μmol kg^{-1}) is calculated from the hysteresis-corrected sensor frequency (F_c) using a modified version of the algorithm by Owens and Millard (1985), in which correction functions are applied to account for the sensor response to temperature and pressure, as well as for the finite sensor response time using the time rate of change of the continuously sampled frequency output (see Sea-Bird Electronics, Inc. 2010b),

$$\text{DO} = \text{Soc}\left[F_c + F_{\text{offset}} + \tau(T,P)\frac{dF}{dt}\right] \times T_{\text{cor}}(T)P_{\text{cor}}(P,T)O_{2\text{sol}}(T,S), \tag{4}$$

where

$$\tau(T,P) = \tau_{20}D_0\exp(D_1P + D_2T), \tag{5}$$

$$T_{\text{cor}}(T) = (1.0 + AT + BT^2 + CT^3), \tag{6}$$

and

$$P_{\text{cor}}(P,T) = \exp[EP/(T + 273)]. \tag{7}$$

Here, T is temperature (°C), S is salinity, and P is the pressure (dbar). Constant coefficients (provided by SBE) A, B, C, and E correct for secondary sensor responses to temperature and pressure. SBE also provides the sensor time constant τ_{20} at 20°C, and compensation coefficients D_0, D_1, and D_2 for the pressure effect on the time constant $\tau(T, P)$; F_{offset} is the sensor output at zero oxygen (provided by Sea-Bird Electronics, Inc.) and $O_{2\text{sol}}(T, S)$ is oxygen saturation as a function of temperature and salinity (Garcia and Gordon 1992). As outlined below, Soc is a linear scaling calibration coefficient, which is a parameter that increases as the sensitivity of the sensor decreases. All of the other constants are taken to be stable parameters of the sensor that neither change with the age of the sensor nor as a result of membrane fouling.

A further processing step is applied to account for the fact that down-going ITP profile measurements can be influenced by the wake of the instrument because the SBE 41CP CTD and SBE 43F DO sensors are mounted in the top hemispherical end cap on the cylindrical pressure case of the ITP. This is evidenced by a smoothing of temperature and salinity fine structure in the down-going profiles that is observed when the ITP drift speed is less than around 15 cm s^{-1} (Krishfield et al. 2008b). It appears that fast ice drift provides horizontal flow that advects the wake downstream of the CTD intake. During down-going profiles, the flow rate through the sensor plumbing is reduced, which in effect shows up as offsets in pressure values of given potential temperature, salinity, or DO surfaces between up- and down-going profiles. To correct for this wake effect, the down-going pressure values are adjusted using a pressure correction based on ITP drift speed, as outlined in Krishfield et al. (2008b). The maximum pressure deviation correction is 3 dbar for a down profile taken when the ice drift speed is zero, which reduces to no correction when the ice drift speed exceeds 30 cm s^{-1}; typical corrections are between 1 and 2 dbar.

Sensor calibration drift can be attributed to fouling and, to a much lesser extent, chemical processes inside the SBE 43F sensor (electrolyte consumption). Sensor drift from electrolyte consumption has been estimated to be less than 0.5% over 1000 h of pumped operation (Janzen et al. 2007). One thousand hours equates to more than 1300 ITP profiles down to 760 m, and so chemical drift does not play a role in our ITP observations. Here, detectable sensor drifts are derived primarily from other sources of drift, such as fouling. Because sensor output is proportional to DO concentration and remains stable in the absence of DO, calibration can be accomplished by adjusting the slope parameter Soc [i.e., applying a single multiplicative correction factor to an entire profile (see Janzen et al. 2007)]. In cases where postdeployment factory calibration is possible, calibrations can be applied if

sensor drift is taken to be linear over time (e.g., Janzen et al. 2007). This is not a possibility here because no ITPs with DO sensors have been recovered for postdeployment calibration.

Reliable calibration procedures have been established for the salinity data collected by ITPs (Krishfield et al. 2008b). Thermistor and pressure sensors on the SBE 41CP CTD are stable over time, while the conductivity sensor drifts and is more susceptible to fouling than the temperature sensor. A calibration procedure is used to correct for small variations in the conductivity measurement for each individual ITP profile (Krishfield et al. 2008b). The procedure assumes that the temperature and pressure measurements are stable, and that at deep potential isotherms the real salinity changes in time are negligible over the course of an ITP deployment. Conductivity sensor drifts are corrected by referencing to bottle-calibrated CTD conductivity on potential temperature surfaces deeper than 500 dbar (deeper than the core of the Atlantic water layer and within the maximum depth range of ITP profiles). ITP oxygen sensor calibration drift is similarly corrected by referencing to mapped fields of ship-derived deep-water oxygen data on potential isotherms. The calibration procedure is based on the assumptions that local DO changes in time are negligible on deep potential isotherms, at least over the course of an ITP deployment. The deep-water DO reference grid (Fig. 1) is derived from pan-Arctic optimal interpolations (OI) of 915 high-quality DO profiles from the 2000s and 164 from the 1990s on a 50-km-square grid [corresponding to the Environmental Working Group (EWG) Atlas; data are available online at http://nsidc.org]. The data sources include profiles from the North Pole Environmental Observatory (NPEO), the Joint Western Arctic Climate Studies (JWACS), the Beaufort Gyre Exploration Project (BGEP), and the Freshwater Switchyard (SWYD) programs; expeditions of the Japanese icebreaker *Mirai*, the Russian icebreaker *Akademik Fedorov*, the Swedish icebreaker *Oden*, and the German icebreaker *Polarstern*; plus additional stations from the World Ocean Data Base. Data are limited to observations since 1990 because we make the simplifying assumption that oxygen distributions on deep isotherms are uniform in time. More information on the basic assumptions of OI and the method can be found in the literature (e.g., Gandin 1965). A covariance length scale necessary for the OI computations was estimated to be 200 km (the correlation of salinity observations on deep isotherms can be approximately represented by a Gaussian function with a length scale of ~200 km). The error in the source measurements was taken to be ± 2 μmol kg^{-1} [based on World Ocean Circulation Experiment (WOCE) standards; e.g., see Culberson et al. (1991)].

A slope correction factor (Fig. 2) for each ITP DO profile is calculated as follows: At three deep potential temperature levels—0.3°, 0.4°, and 0.5°C (which correspond to depths between about 700 and 550 m)—ratios of ITP DO measurements to OI DO grid values are calculated. The slope correction factor is computed by taking a weighted average of the three ratios, with increasing emphasis on the deeper levels presumed to be most stable (three parts from the 0.3°C surface, two parts from 0.4°C, and one part from the 0.5°C potential temperature surface). This factor, effectively a correction to the factory-provided Soc for a given sensor, is multiplied by the entire DO profile.

In general, the calibrations are relatively stable, with anomalous values persisting over multiple profiles that can be attributed to sensor fouling (Fig. 2). For ITPs 23 and 29, intermittent deviations from calibration were observed early on in their deployment, between October and December 2008 (between about 30 and 140 days after deployment; see Fig. 2). Although we cannot determine the cause of these shifts in sensor output exactly, we hypothesize that these might reflect fouling events, such as those that might be expected from detrital ice algae detaching from the ice at the end of the growing season. However, it is difficult to test such scenarios without corroborating bio-optical data.

Observed calibration drifts of the sensors are up to 10% over 1 yr, greatly exceeding what is expected from electrolyte conversion alone. After a sensor drift exceeded about 7%–8%, the DO data exhibited more spikes and higher noise levels. This is the case for the sensor on ITP 6 after about 382 days of operation (765 profiles) and for ITP 13, after about 648 profiles. Note also that after about 170 days (340 profiles), the sensor on ITP 6 shows differences between successive up and down profile correction factors of up to 2% for reasons that are unclear. A pump variation does not appear to be responsible because conductivity cell correction factors do not vary between up and down profiles.

3. Observations

The four ITP systems equipped with DO sensors drifted in the Canada and Makarov Basins between 2006 and 2009, providing 3385 high-quality profiles of DO concentration, salinity, and temperature between 5 September 2006 and 23 December 2009 (Fig. 3 and Table 1). All ITPs returned 2 one-way profiles per day, initiated at 0000 and 0600 UTC. ITP 6 (13) profiled between 9 (7)- and 760-m depths in the Canada Basin, while ITPs 23 and 29, deployed in August 2008, were still profiling between 7- and 760-m depths at the time of writing; their drift tracks span the Canada and Makarov Basins (Table 1).

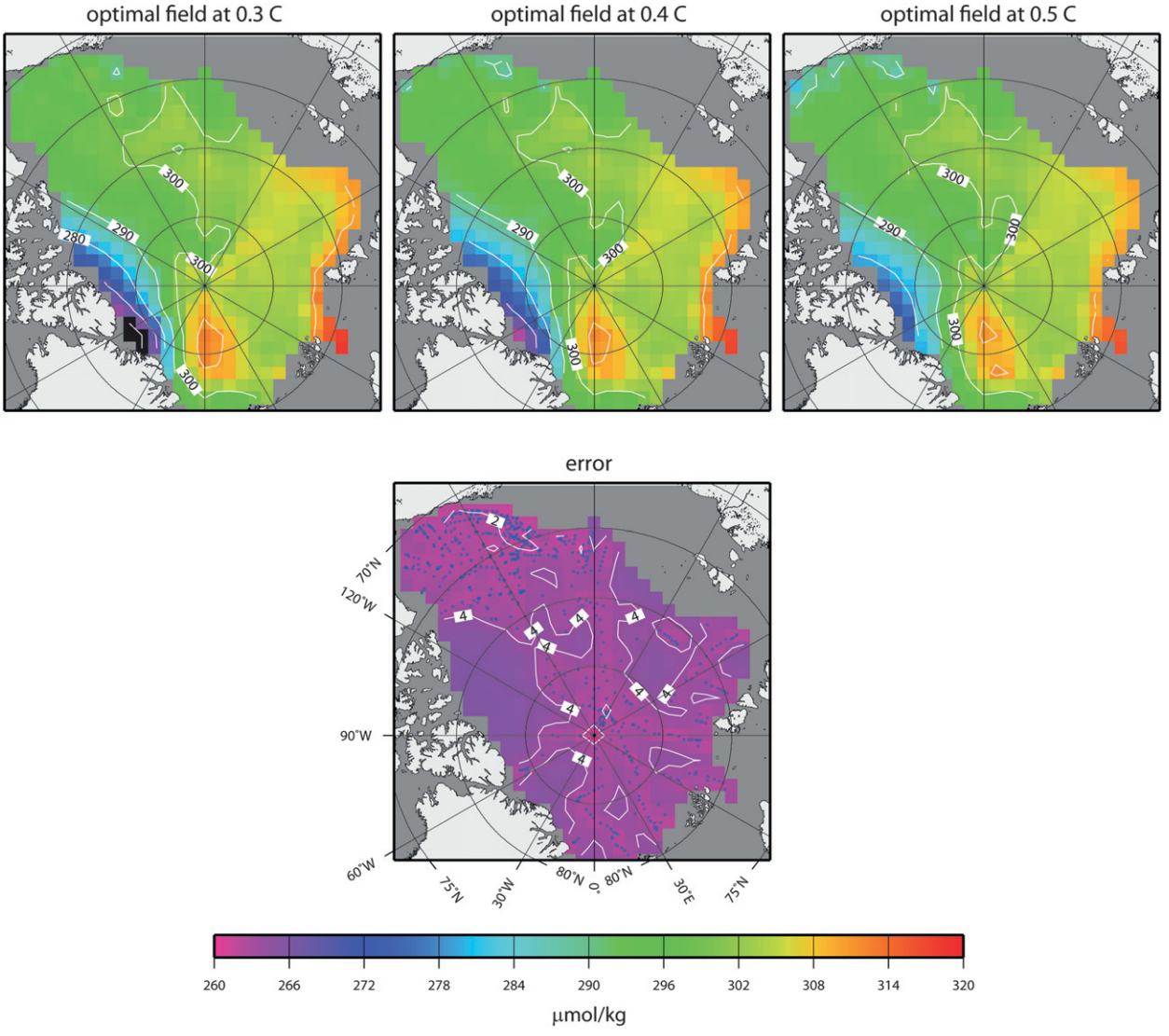

FIG. 1. (top) Dissolved oxygen from optimal interpolation of calibrated ship observations on (left) $\theta = 0.3°C$, (middle) 0.4°C, and (right) 0.5°C. (bottom) The estimated error of the interpolation, generally <4 μmol kg^{-1}, and <6 μmol kg^{-1} where the grid is not well constrained because of sparse data coverage. The locations of DO profiles used to construct the OI grid are indicated in the bottom panel (dots). Note that the relatively low DO values in the region north of the Canadian Archipelago mark less well-ventilated waters farthest from the incoming Atlantic Water boundary current (see Falkner et al. 2005).

The ITPs drift as the perennial ice pack moves. Typical ice drift speeds are around 10 cm s^{-1}, which implies a typical horizontal ITP survey resolution of about 6 km for profiles taken 18 h apart.

DO values plotted against salinity and depth (Fig. 4) demonstrate the effectiveness of using profile-dependent multiplicative adjustments to match ITP DO on deep potential temperature surfaces to a spatially varying reference field. Profiles are typically characterized by saturated or supersaturated values in the surface mixed layer of the Arctic Ocean, which is generally shallower than about 40 m in the survey region. Below the mixed layer, oxygen concentrations typically decrease with depth to minima at salinities between about 32.5 and 33.7 (around 100–200 m). These minima (DO saturations of about 60%–75%) are associated with waters of Pacific origin that have low oxygen levels, presumably because of respiratory activity in the microbial assemblage (Falkner et al. 2005). At greater depth the Atlantic water layer, with a core depth of around 400 m, is relatively well ventilated, with DO saturations of about 85%. This is evident also in the shipboard data that indicate the highest DO are where the Atlantic water enters the Eurasian Basin, and lower

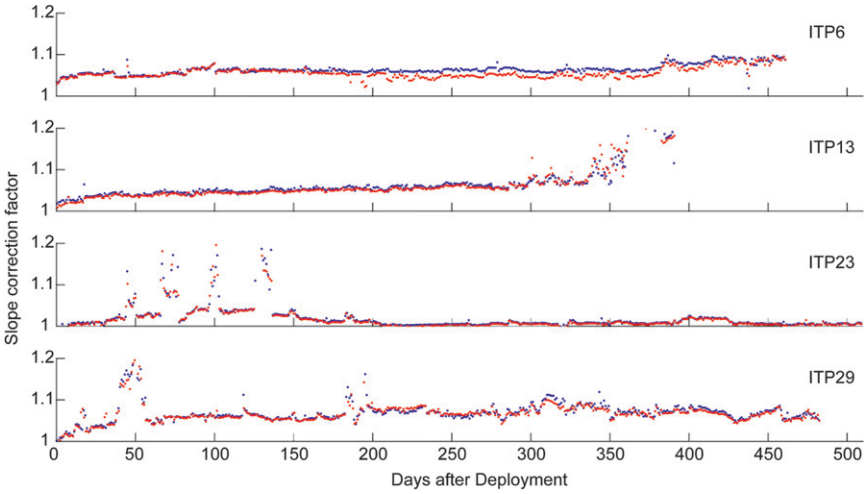

FIG. 2. Time series of SBE 43F slope correction factor [down profile (red) and up profile (blue)] for each ITP based on optimal interpolation grids. Each ITP returned 2 one-way DO profiles per day.

values are found farther downstream in the Canadian Basin (Fig. 1).

Difficulties arise when using drifting buoy data to examine DO in the variable surface waters. Distinguishing spatial variability from temporal variability is complicated by the fact that the buoys often drift over large areas across major upper-ocean water mass boundaries over the course of a seasonal cycle. This further complicates the ability to distinguish between the advective and in situ contributions to DO concentration, which is already difficult in the Arctic because of variable sea ice coverage (and, hence, strong regional and temporal differences in light penetration and air–sea gas exchange). It should also be pointed out that the ITP does not sample shallower than about 5–7 m below the underside of the ice, and that in the summer months the surface mixed layers in July and August can be thinner than the shallowest ITP measurement (Toole et al. 2010). Despite these limitations, pronounced spatial and seasonal characteristics of DO in the upper-water column can be

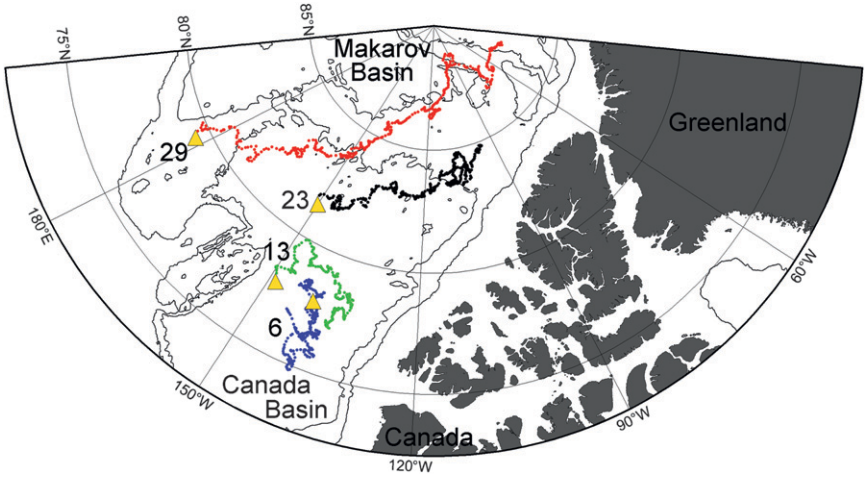

FIG. 3. Drift tracks of ITPs 6, 13, 23, and 29 used in our analysis. Although ITPs 6 and 13 continued to operate beyond the tracks shown here, oxygen data were unreliable because of what appears to be excessive sensor fouling (DO on deep isotherms differs from climatology by more than about 8%, while noise levels and spikes in the data record increase significantly). The start of each drift track (yellow triangles) is shown. The 1000- and 2500-m isobaths have been plotted using the IBCAO grid (online at http://www.ibcao.org/). (See http://www.whoi.edu/itp for the current status of ITPs 23 and 29, still operating as of this writing.)

TABLE 1. ITPs incorporating dissolved oxygen sensors (see http://www.whoi.edu/itp for the current status of ITPs 23 and 29, still operating at the time of writing). ''End date'' corresponds to the last DO profile used in the analysis here.

ITP No.	Start position	Start date	End date	Total DO profiles
6	77.9°N, 140.4°W	5 Sep 2006	22 Sep 2007	765
13	78.0°N, 149.2°W	13 Aug 2007	26 May 2008	648
23	81.7°N, 150.9°W	5 Aug 2008	23 Dec 2009	1014
29	79.5°N, 177.3°W	30 Aug 2008	23 Dec 2009	958

identified. In the following subsections, some potential analyses of DO from ITP-mounted sensors are demonstrated by drawing attention to several ocean features observed in the data.

a. Water mass boundaries

There is significant spatial variability in surface ocean (mixed layer) temperature, salinity, and DO values over the survey region (Fig. 5). Surface mixed-layer depth was calculated to be where the potential density relative to 0 dbar first exceeded the shallowest sampled density by 0.01 kg m^{-3} (see Toole et al. 2010). Quantities plotted in Fig. 5 are an average of values within the mixed layer of each profile (mixed layer depth ranges between about 10 and 45 m, depending on season and location). ITP 23 transected a major water mass front in December 2008 that possibly delineates the northern extension of the oceanic Beaufort Gyre at about 83°N, 129°W (Fig. 6; also, note the arrows in Fig. 5). Water masses on either side of the front have different physical, chemical, and biological properties, and ITPs provide a means to monitor how these properties change spatially and temporally, which is a leading question in the context of Arctic climate. ITP 23 crossed the front passing from relatively warm, fresh surface water to the southwest and colder, saltier surface water to the northeast. Spatial variability appears to dominate temporal change in this record because time–depth sections (not shown) of the indirect ITP track are very similar to the distance–depth section. The mixed layer to the north is more characteristic of the Eurasian winter mixed layer (thicker than the Canadian winter mixed layer), with salinities in the range of $29 \lesssim S \lesssim 30$ (see, e.g., Steele et al. 2004; Timmermans et al. 2008). The highest DO concentrations arise at the surface on the northern side of the front. DO percent saturation changes across the front accordingly, indicating that differences do not result from solubility changes. Also on the northern side of the front, changes in DO (and DO percent saturation) generally follow changes in salinity, with DO increasing with salinity and vice versa (this relationship is not discernable in Fig. 5 because

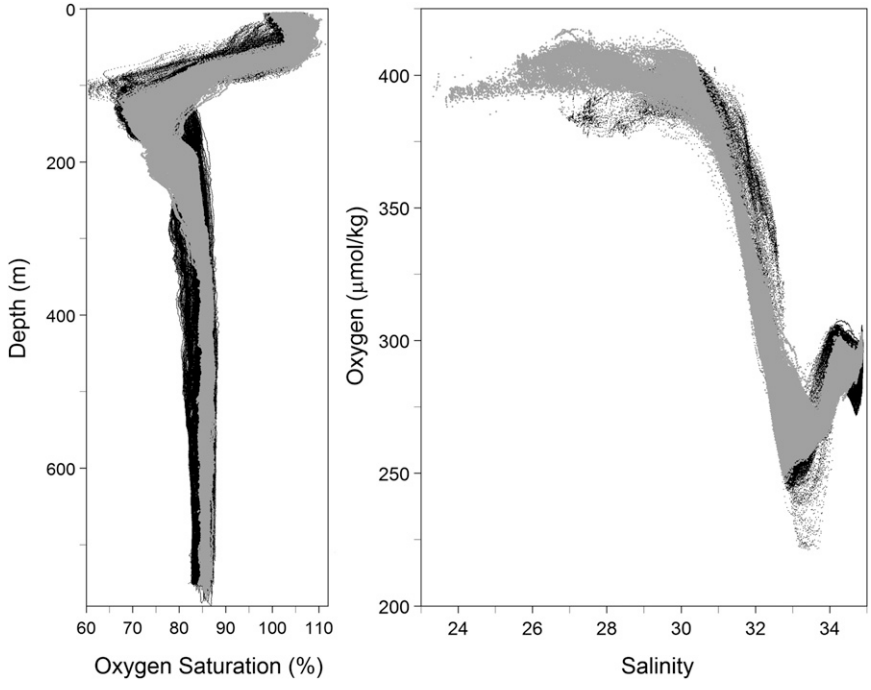

FIG. 4. Dissolved oxygen data from ITPs 6 and 13 (gray), and 23 and 29 (black) as functions of (left) depth (DO percent saturation) and (right) salinity (DO). For clarity, only the up profiles are shown here. The spread of data points indicates spatial variability (with some temporal variability near the surface).

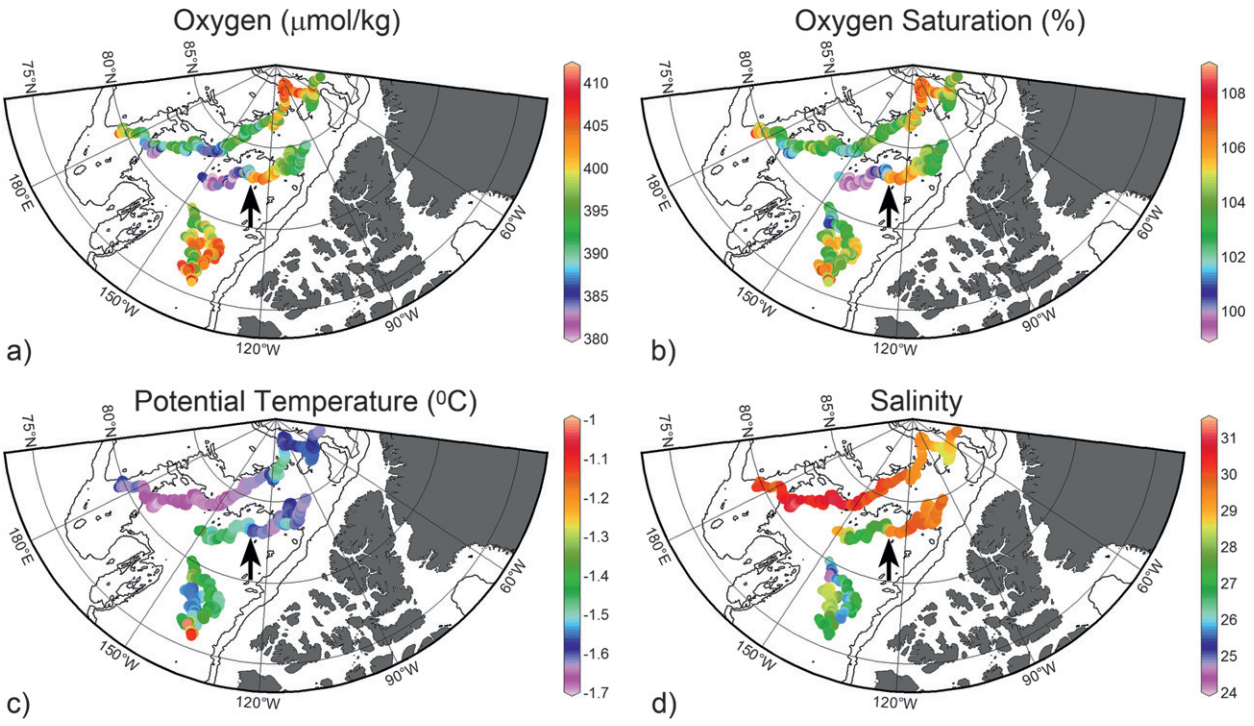

FIG. 5. Maps of (a) dissolved oxygen, (b) oxygen percent saturation, (c) potential temperature, and (d) salinity in the surface mixed layer (see text) measured by ITPs 6, 13, and 23 and ITP 29 between 5 Sep 2006 and 23 Dec 2009. Values are not plotted if the mixed layer depth was either within 2 m of the shallowest depth sampled by the ITP or was <10 m (i.e., if the shallowest depth sampled did not reach the surface mixed layer; primarily these are profiles from ITPs 6 and 13 in July and August 2007 when the mixed layer is thinner than 10 m). The arrows in each panel mark the crossing of a water mass front by ITP 23.

changes in salinity on the northern side of the front are relatively small compared to salinity variations over the entire survey region). This may be attributed to biological and physical processes, discussed in the next section.

On the southern side of the front, surface waters are relatively oxygen depleted compared to the central Canada Basin, even though temperature and salinity values are similar. Surface DO in the region of the first half of ITP 23 track is consistently around 100% saturation with no trends, indicating efficient equilibration with the atmosphere (possibly suggesting nearby open water or advection from open regions), stable ice conditions (no growth or decay), balanced respiration–photosynthesis (between spring and fall), or higher mixing and entrainment of deeper oxygen-depleted waters. Note also that a subsurface DO maximum between 20 and 50 m persists between August 2008 and December 2008 (when the ITP crosses the front); a similar feature will be discussed in the next section where regions of the ITP drift tracks within one water mass region are considered in order to assess temporal variability.

b. Seasonal evolution of DO

The upper-water column, which is shallower than about 70 m, is most affected by seasonal processes. Over the seasons, DO concentrations in the ice-covered upper ocean are affected by biological production and consumption, oxygen exchange upon ice melt and freezing, partial equilibration with the atmosphere depending on the proximity of leads and open water, and mixing with deeper waters.

In contrast to ITP 23, observed changes appear to be predominantly temporal over much of the drift of ITP 13 in a localized region of the central Canada Basin. Between August and December a prominent shallow DO maximum is observed immediately below the surface mixed layer (Fig. 7; see also Sherr and Sherr 2003). This DO maximum is likely the result of accumulation of oxygen in the surface water in summer by in situ photosynthetic oxygen production. DO is prevented from escaping to the atmosphere by strong surface stratification (a summer halocline) that is formed as a result of surface freshening by ice melt. The maximum is destroyed in winter by convection and deepening of the surface layer induced by brine rejection and increased ice–ocean stresses [with some reduction also possible by respiration (Sherr and Sherr 2003)]. Note also the presence of a near-surface temperature maximum (NSTM) underlying the surface mixed layer (Fig. 7). The NSTM is believed to be formed when solar radiation penetrates the surface ocean through

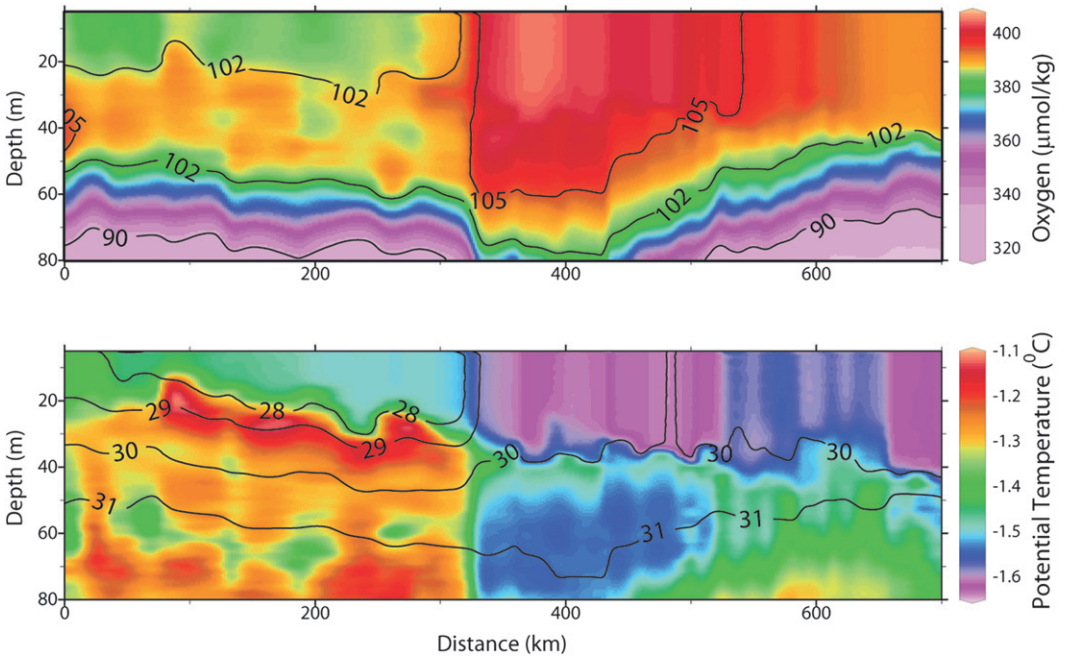

FIG. 6. Distance–depth section of (top) dissolved oxygen (contour lines indicate percent saturation) and (bottom) potential temperature (contour lines indicate salinity) measured by ITP 23. The section was constructed by mapping the profile data onto a straight line from the start to the end of the drift track shown in Fig. 3.

open water (e.g., leads) in summer and becomes trapped below the surface by the formation of the summer halocline (Maykut and McPhee 1995; McPhee et al. 1998; Jackson et al. 2010; Toole et al. 2010).

Another important feature arises in the surface water as the season progresses with high DO in the winter months, well after photosynthetic activity has ceased. In February and March, a maximum in DO supersaturation

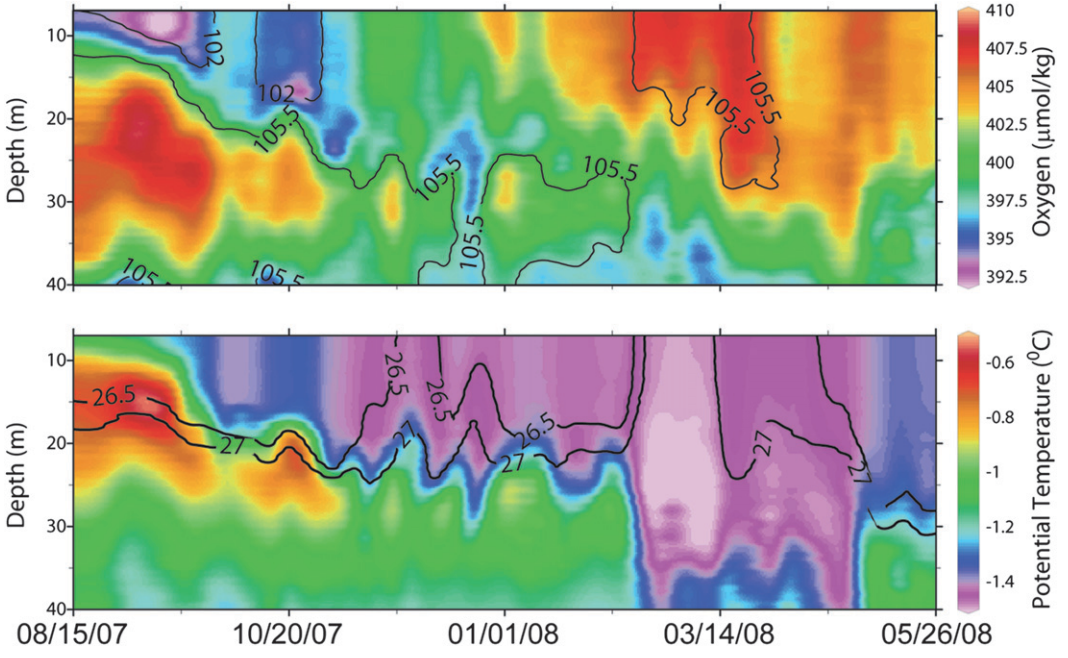

FIG. 7. The evolution of (top) dissolved oxygen (contour lines indicate percent saturation) and (bottom) potential temperature (contour lines indicate salinity) in the upper 40 m in the central Canada Basin as measured by ITP 13.

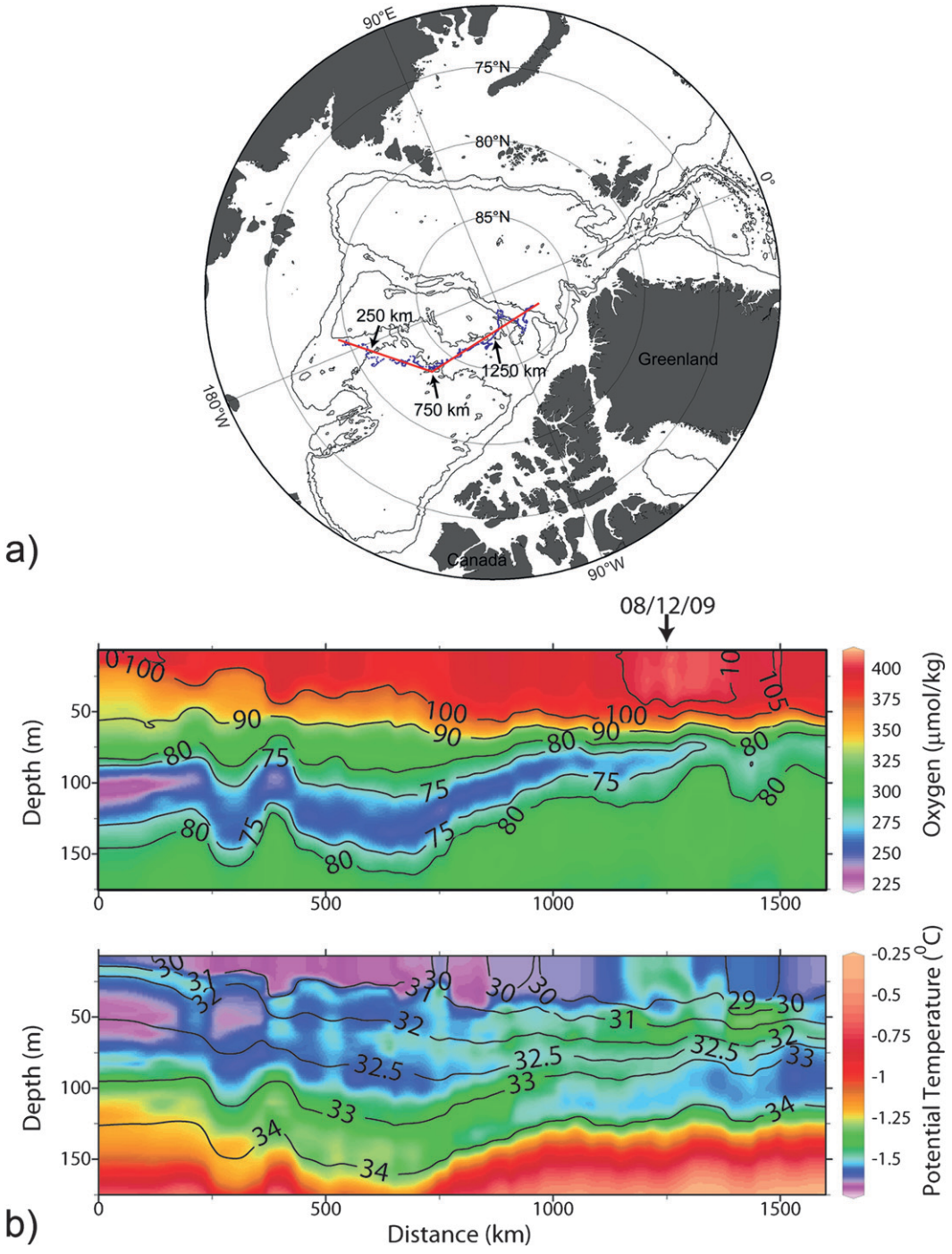

FIG. 8. (a) Map showing the drift track of ITP 29 (between 31 Aug 2008 and 22 Dec 2009) and the straight lines onto which the profile data were mapped to make (b) the sections of (top) dissolved oxygen (contour lines indicate percent saturation) and (bottom) potential temperature (contour lines indicate salinity). Water of Pacific origin is indicated by a marked DO minimum on $S \approx 33$. Note that seasonal variability in the surface mixed layer is also measured in the form of high DO supersaturation in July–September (see the date marked in the top section), indicating summer ice algal and phytoplankton production (cf. Codispoti and Richards 1971); corresponding temperature and salinity are warmer and fresher.

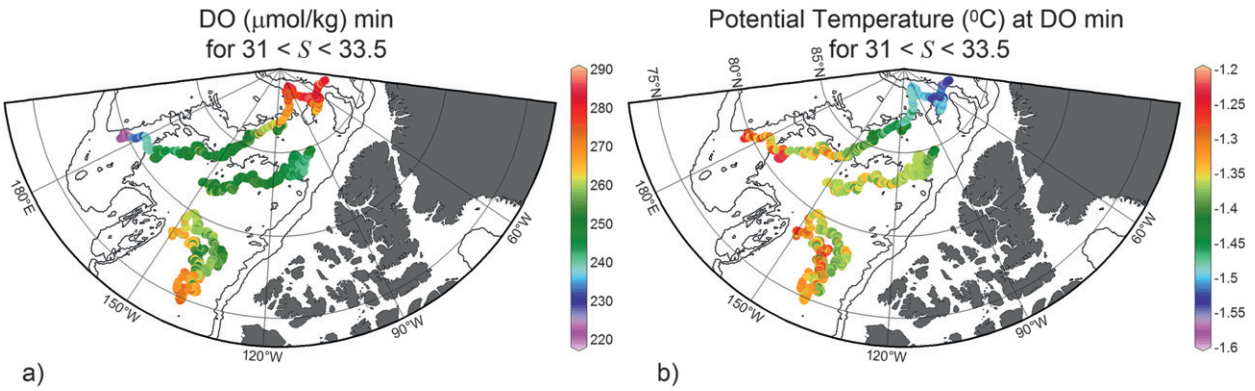

FIG. 9. Maps showing the (a) DO minimum over the salinity range of halocline water of Pacific origin $31 < S < 33.5$ and (b) corresponding potential temperature.

is observed with corresponding high salinities and cold temperatures (Fig. 7). This can be likely attributed to the exclusion of gas from the ice lattice as water freezes, and has been observed at the ice–water interface both in the Arctic Ocean (e.g., Top et al. 1985) and in ice-covered lakes in Antarctica (e.g., Hood et al. 1998). Extensive winter ice cover prevents the excess oxygen from escaping to the atmosphere. Hence, DO changes in the surface ocean reflect physical processes in addition to biological primary production. In this example, spatial variability is also evident: after March there is a rather rapid decrease in salinity and mixed-layer depth that is not consistent with time evolution under a freezing ice cover. Future deployments of DO sensors on ITPs in close proximity to ice mass balance buoys (IMB) making concurrent measurements of ice growth will allow us to clarify the impact of ice growth–melt on surface water DO.

c. *Pacific water*

Pacific water is a key nutrient, freshwater, and heat source to the Arctic (Woodgate and Aagaard 2005); it has a distinct low DO signature, making DO an important tracer for understanding Pacific water dynamics and pathways (Falkner et al. 2005). The lowest DO values surveyed by the ITPs are found on the $S \approx 33$ isohaline (around 100-m depth) in the westernmost part of the survey region over the Mendeleyev Ridge at the start of the ITP 29 drift (Figs. 8 and 9). The prominent DO minimum diminishes as the ITP crosses the Alpha Ridge between the Canada and Makarov Basins. This pattern in general is agreement with the summer Bering Seawater circulation in the Arctic Ocean inferred by Steele et al. (2004) using potential temperature and salinity. A map of minimum DO over the salinity range for halocline water of Pacific origin (Fig. 9a), which can be taken to be approximately $31 < S < 33.5$ (see Shimada et al. 2005; Steele et al. 2004), shows a clear front between low DO minima and higher values on the northern side of the Alpha Ridge (the front is evident also in the lateral gradient of corresponding potential temperature; see Fig. 9b). The maps suggest that in 2008–09 Pacific water was swept eastward into the anticyclonic Beaufort Gyre centered in the Canada Basin, likely in response to basin-scale wind patterns (cf. Steele et al. 2004); the Transpolar Drift Stream, which can carry Pacific Water northward directly across the Arctic from the Bering Sea, had significantly reduced strength in 2009 (Proshutinsky et al. 2010). These and future deployments of DO sensors on ITPs will provide useful year-round tracer measurements of Pacific Water to resolve relationships between Pacific Water influxes and surface wind patterns associated with atmospheric climate modes.

d. *Eddies*

The horizontal ITP survey resolution of a few kilometers has made the discovery of cold-core eddies prevalent below the surface mixed layer possible (with center depths around 50 m and horizontal scales on the order of 10 km) in the central Canada Basin (Timmermans et al. 2008). Such eddies cannot be resolved by typical ice breaker hydrographic surveys that have station spacings on the order of tens of kilometers. Timmermans et al.'s (2008) analysis of ITP temperature and salinity measurements through 21 eddies suggests that approximately 10% of the central Canada Basin may be covered by shallow eddies, possibly having a significant impact on mixing and heat transfer in the halocline. Eddy properties are consistent with their formation by the instability of a surface front (Timmermans et al. 2008), which is the same front transected by ITP 23. One of these eddies was sampled by ITP 6 between 19 and 25 September 2006 (Fig. 10), so that DO measurements were available in addition to temperature and salinity. Anomalously high

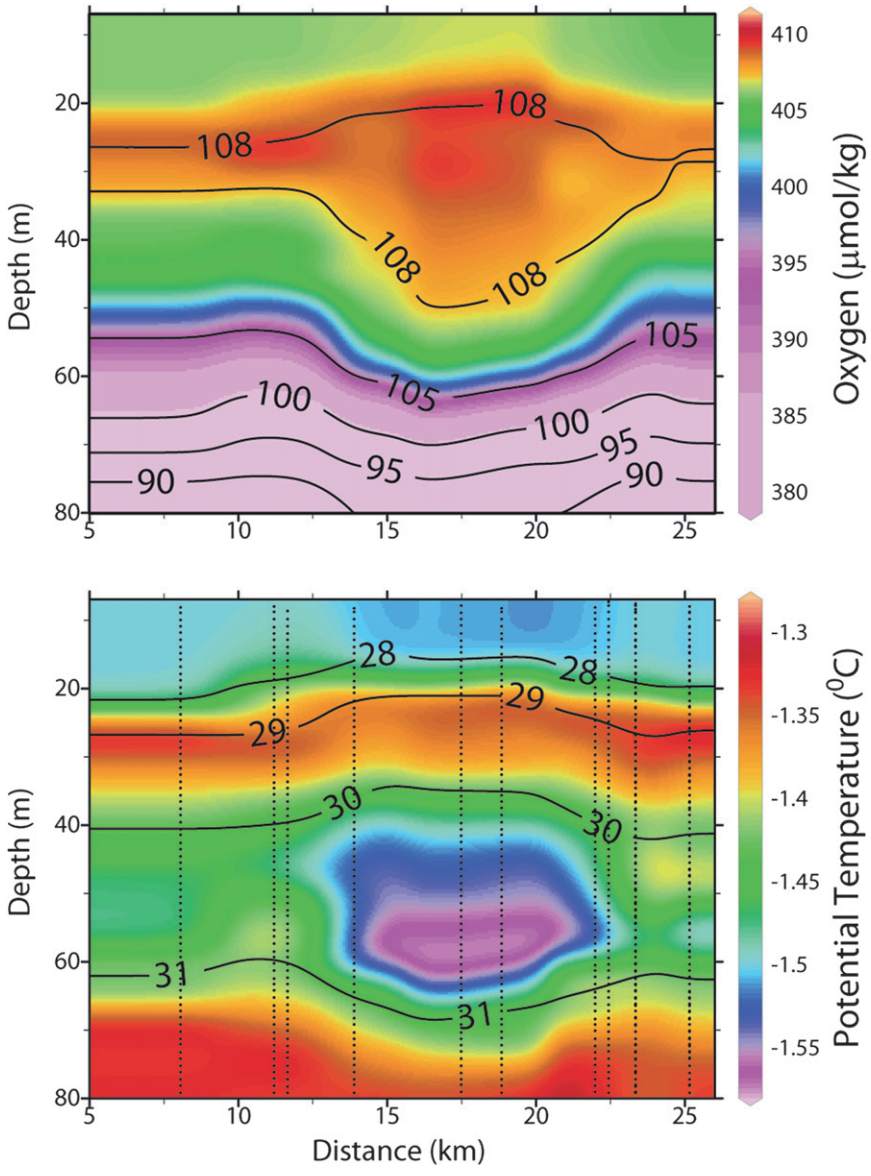

FIG. 10. Sections of (top) dissolved oxygen (contour lines indicate percent saturation) and (bottom) potential temperature (contour lines indicate salinity) through a cold-core eddy transected by ITP 6 in the central Canada Basin (near 78°N, 140°W) in September 2006. Dotted lines in the bottom panel indicate ITP profile locations.

DO in the core of the eddy further confirms the hypothesis that the shallow eddies transected by ITPs on the southern side of the surface front are derived from water that is subducted from the relatively dense, high DO surface water on the northern side of the front.

4. Summary and discussion

Dissolved oxygen sensors on ITPs in the Arctic Ocean have provided year-round DO measurements from the surface mixed layer to 760-m depth under permanent ice cover. Initial results indicate the exceptional potential of such measurements for contributing valuable, unique information on Arctic Ocean circulation, dynamics, ecology, and biogeochemistry on seasonal-to-interannual time scales. First results attest to the effectiveness of ITPs in measuring across water mass boundaries by the crossing of a major water mass front, demonstrating a decoupling between ice drift and surface ocean processes. Year-round time series measurements by these ITPs exhibit seasonal changes in surface water DO that appear to reflect both biological primary production as well as the physical process of ice growth and melting. DO

concentrations in the surface ocean are generally saturated or supersaturated as a result of the trapping of excess DO (either photosynthetically produced or injected by the exclusion of dissolved gas by growing ice) by the ice cover. DO sensors on ITPs exhibit the possibility for basin-wide studies of Pacific water, a major water mass in the Arctic Ocean that can be identified by its distinctive DO properties. On much smaller scales, features such as eddies can be well resolved by the high-resolution ITP sampling, while DO measurements can be extremely valuable in ascertaining their origin and dynamics.

DO is strongly locally dependent on ice concentration because partial equilibration with the atmosphere takes place in the vicinity of leads and open water. Changes in snow cover and ice thickness also affect DO concentrations by their influence on under-ice light levels, impacting under-ice photosynthesis. Future studies will require the integration of DO measurements with simultaneous ice thickness and concentration data, as well as measurements of under-ice light levels and in situ proxies for phytoplankton biomass, such as chlorophyll fluorescence, to better assess the biological contributions to DO variability. Further studies could also utilize methods based on concurrent measurements of dissolved nitrogen, oxygen, and argon to distinguish biological from physical contributions to DO concentrations. National Science Foundation funding is in place for the deployment of three additional ITPs per year (through 2014) that will be equipped with DO sensors and distributed throughout the Arctic Ocean.

Acknowledgments. The National Science Foundation Office of Polar Programs Arctic Sciences Section under Awards ARC-0519899, ARC-0856479, and ARC-0806306 provided funding. The Woods Hole Oceanographic Institution Arctic Research Initiative also provided support. Thank you to Andrey Proshutinsky for helpful comments. We appreciate the support of the captain and crew of the Canadian Coast Guard icebreaker *Louis S. St-Laurent*, and we acknowledge financial and ship time support from Fisheries and Oceans Canada, the Canadian International Polar Year Program's Canada's Three Oceans project, and the U.S. National Science Foundation's Beaufort Gyre Exploration Project, and collaboration with the Japan Agency for Marine-Earth Science and Technology. Ocean Data View software was used in this work (R. Schlitzer, Ocean Data View, 2009; available online at http://odv.awi.de).

REFERENCES

Arrigo, K. R., G. L. van Dijken, and S. Pabi, 2008: The impact of a shrinking Arctic ice cover on marine primary production. *Geophys. Res. Lett.,* **35,** L19603, doi:10.1029/2008GL035028.

Bopp, L., C. Le Quéré, M. Heimann, A. C. Manning, and P. Monfray, 2002: Climate-induced oceanic oxygen fluxes: Implications for the contemporary carbon budget. *Global Biogeochem. Cycles,* **16,** 1022, doi:10.1029/2001GB001445.

Codispoti, L., and F. Richards, 1971: Oxygen supersaturations in the Chukchi and East Siberian Seas. *Deep-Sea Res.,* **18,** 341–351.

——, C. Flagg, and V. Kelly, 2005: Hydrographic conditions during the 2002 SBI process experiments. *Deep-Sea Res. II,* **52,** 3199–3226, doi:10.1016/j.dsr2.2005.10.007.

Cota, G. F., L. R. Pomeroy, W. G. Harrison, E. P. Jones, F. Peters, W. M. Sheldon, and T. R. Weingartner, 1996: Nutrients, primary production and microbial heterotrophy in the southeastern Chukchi Sea: Arctic summer nutrient depletion and heterotrophy. *Mar. Ecol. Prog. Ser.,* **135,** 247–258.

Culberson, C. H., G. Knapp, M. Stalcup, R. T. Williams, and F. Zemlyak, 1991: A comparison of methods for the determination of dissolved oxygen in seawater. WHP Office Rep. WHPO 91-2, WOCE Rep. 73/91, 77 pp.

Edwards, B., D. Murphy, C. Janzen, and N. Larson, 2009: Calibration, response and hysteresis in deep sea dissolved oxygen measurements. *J. Atmos. Oceanic Technol.,* **27,** 920–931.

Falkner, K., M. Steele, R. Woodgate, J. Swift, K. Aagaard, and J. Morison, 2005: Dissolved oxygen extrema in the Arctic Ocean halocline from the North Pole to the Lincoln Sea. *Deep-Sea Res. I,* **52,** 1138–1154.

Gandin, L. S., 1965: *Objective Analysis of Meteorological Fields*. U.S. Department of Commerce and National Science Foundation, 242 pp.

Garcia, H. E., and L. I. Gordon, 1992: Oxygen solubility in seawater: Better fitting equations. *Limnol. Oceanogr.,* **37,** 1307–1312.

Gruber, N., and Coauthors, 2009: Adding oxygen to Argo: Developing a global in-situ observatory for ocean deoxygenation and biogeochemistry. *Proc. OceanObs'09 Conf.,* Venice, Italy, OC/UNESCO and Cosponsors. [Available online at http://www.oceanobs09.net/blog/?p=665.]

Hood, E. M., B. L. Howes, and W. J. Jenkins, 1998: Dissolved gas dynamics in perennially ice-covered Lake Fryxell, Antarctica. *Limnol. Oceanogr.,* **43,** 265–272.

Itoh, M., E. Carmack, K. Shimada, F. McLaughlin, S. Nishino, and S. Zimmermann, 2007: Formation and spreading of Eurasian source oxygen-rich halocline water into the Canadian Basin in the Arctic Ocean. *Geophys. Res. Lett.,* **34,** L08603, doi:10.1029/2007GL029482.

Jackson, J. M., E. C. Carmack, F. A. McLaughlin, S. E. Allen, and R. G. Ingram, 2010: Identification, characterization, and change of the near-surface temperature maximum in the Canada Basin, 1993–2008. *J. Geophys. Res.,* **115,** C05021, doi:10.1029/2009JC005265.

Janzen, C., D. Murphy, and N. Larson, 2007: Getting more mileage out of dissolved oxygen sensors in long-term moored applications. *Proc. Oceans 2007,* Vancouver, BC, Canada, IEEE, doi:10.1109/OCEANS.2007.4449398.

Johnson, G. C., and N. Gruber, 2007: Decadal water mass variations along 20°W in the northeastern Atlantic Ocean. *Prog. Oceanogr.,* **73,** 277–295, doi:10.1016/j.pocean.2006.03.022.

——, J. M. Toole, and N. G. Larson, 2007: Sensor corrections for Sea-Bird SBE-41CP and SBE-41 CTDs. *J. Atmos. Oceanic Technol.,* **24,** 1117–1130.

Kinney, P., M. E. Arhelger, and D. C. Burrell, 1970: Chemical characteristics of water masses in the Amerasian Basin of the Arctic Ocean. *J. Geophys. Res.,* **75,** 4097–4104.

Krishfield, R., J. Toole, A. Proshutinsky, and M.-L. Timmermans, 2008a: Automated ice-tethered profilers for seawater observations

under pack ice in all seasons. *J. Atmos. Oceanic Technol.,* **25,** 2091–2095.

——, ——, and M.-L. Timmermans, 2008b: ITP data processing procedures. Woods Hole Oceanographic Institution Tech. Rep., 24 pp. [Available online at http://www.whoi.edu/fileserver.do?id=35803&pt=2&p=41486.]

Maykut, G. A., and M. G. McPhee, 1995: Solar heating of the Arctic mixed layer. *J. Geophys. Res.,* **100** (C12), 24 691–24 703.

McLaughlin, F., E. Carmack, R. Macdonald, H. Melling, J. Swift, P. Wheeler, B. Sherr, and E. Sherr, 2004: The joint role of Pacific and Atlantic-origin waters in the Canada Basin, 1997–1998. *Deep-Sea Res. I,* **51,** 107–128.

McPhee, M. G., T. P. Stanton, J. H. Morison, and D. G. Martinson, 1998: Freshening of the upper ocean in the Arctic: Is perennial sea ice disappearing? *Geophys. Res. Lett.,* **25,** 1729–1732.

Mecking, S., C. Langdon, R. A. Feely, C. L. Sabine, C. A. Deutsch, and D.-H. Min, 2008: Climate variability in the North Pacific thermocline diagnosed from oxygen measurements: An update based on the U.S. CLIVAR/CO_2 Repeat Hydrography cruises. *Global Biogeochem. Cycles,* **22,** GB3015, doi:10.1029/2007GB003101.

Nihoul, J. C. J., and A. G. Kostianoy, Eds., 2009: *Influence of Climate Change on the Changing Arctic and Sub-Arctic Conditions.* NATO Science for Peace and Security Series, Subseries C: Environmental Security, Springer-Verlag, 226 pp.

Owens, W. B., and R. C. Millard Jr., 1985: A new algorithm for CTD oxygen calibration. *J. Phys. Oceanogr.,* **15,** 621–631.

Pomeroy, L. R., 1997: Primary production in the Arctic Ocean estimated from dissolved oxygen. *J. Mar. Syst.,* **10,** 1–8.

Proshutinsky, A., and Coauthors, 2009: Ocean. Arctic Report Card: Update for 2009. [Available online at http://www.arctic.noaa.gov/reportcard/ocean.html.]

——, and Coauthors, 2010: The Arctic Ocean. *Bull. Amer. Meteor. Soc.,* **91,** S109–S112.

Richter-Menge, J., and J. E. Overland, Eds., 2009: Arctic Report Card: Update for 2009. [Available online at http://www.arctic.noaa.gov/reportcard/index.html.]

Riser, S. C., and K. S. Johnson, 2008: Net production of oxygen in the subtropical ocean. *Nature,* **451,** 323–325.

Sea-Bird Electronics, Inc., 2010a: SBE 43 dissolved oxygen sensor—Background information, deployment recommendations, and cleaning and storage. Application Note 64, 8 pp. [Available online at http://www.seabird.com/pdf_documents/ApplicationNotes/appnote64Feb10.pdf.]

——, 2010b: SBE 43 dissolved oxygen sensor calibration and data corrections using Winkler titrations. Application Note 64-2, 10 pp. [Available online at http://www.seabird.com/pdf_documents/ApplicationNotes/Appnote64-2Feb10.pdf.]

——, 2010c: SBE 43 dissolved oxygen (DO) sensor—Hysteresis corrections. Application Note 64-3, 7 pp. [Available online at http://www.seabird.com/pdf_documents/ApplicationNotes/appnote64-3Feb10.pdf.]

Sherr, B., and E. Sherr, 2003: Community respiration/production and bacterial activity in the upper water column of the central Arctic Ocean. *Deep-Sea Res. I,* **50,** 529–542.

Shimada, K., M. Itoh, S. Nishino, F. McLaughlin, E. Carmack, and A. Proshutinsky, 2005: Halocline structure in the Canada Basin of the Arctic Ocean. *Geophys. Res. Lett.,* **32,** L03605, doi:10.1029/2004GL021358.

Steele, M., J. Morison, W. Ermold, I. Rigor, and M. Ortmeyer, 2004: Circulation of summer Pacific halocline water in the Arctic Ocean. *J. Geophys. Res.,* **109,** C02027, doi:10.1029/2003JC002009.

Stramma, L., G. C. Johnson, J. Sprintall, and V. Mohrholz, 2008: Expanding oxygen-minimum zones in the tropical oceans. *Science,* **320,** 655–658.

Timmermans, M.-L., J. Toole, A. Proshutinsky, R. Krishfield, and A. Plueddemann, 2008: Eddies in the Canada Basin, Arctic Ocean, observed from ice-tethered profilers. *J. Phys. Oceanogr.,* **38,** 133–145.

Toole, J. M., M.-L. Timmermans, D. K. Perovich, R. A. Krishfield, A. Proshutinsky, and J. A. Richter-Menge, 2010: Influences of the ocean surface mixed layer and thermohaline stratification on Arctic sea ice in the central Canada Basin. *J. Geophys. Res.,* **115,** C10018, doi:10.1029/2009JC005660.

Top, Z., S. Martin, and P. Becker, 1985: On the dissolved surface oxygen supersaturation in the Arctic. *Geophys. Res. Lett.,* **12,** 821–823.

Woodgate, R. A., and K. Aagaard, 2005: Revising the Bering Strait freshwater flux into the Arctic Ocean. *Geophys. Res. Lett.,* **32,** L02602, doi:10.1029/2004GL021747.

——, ——, J. H. Swift, K. K. Falkner, and W. M. Smethie Jr., 2005: Pacific ventilation of the Arctic Ocean's lower halocline by upwelling and diapycnal mixing over the continental margin. *Geophys. Res. Lett.,* **32,** L18609, doi:10.1029/2005GL023999.